Interaction of hematopoietic CD34+ CD45+ stem cells and cancer cells stimulated by TGF-β1 in a model of glioblastoma *in vitro*

ELENA MILKINA[1,2], ARINA PONOMARENKO[1,2], MARIA KORNEYKO[1], IRINA LYAKHOVA[1], YULIA ZAYATS[1], SERGEY ZAITSEV[1], POLINA MISCHENKO[1,2], MARINA ELISEIKINA[2], YURI KHOTIMCHENKO[1,2], VALERYI SHEVCHENKO[1,3], HARI SHARMA[4] and IGOR BRYUKHOVETSKIY[1,2]

[1]School of Biomedicine of The Far Eastern Federal University, Vladivostok 690091; [2]National Scientific Center of Marine Biology FEB RAS, Vladivostok 690041; [3]N.N. Blokhin Russian Cancer Research Center, Moscow 115478, Russia; [4]International Experimental CNS Injury & Repair (IECNSIR), Department of Surgical Sciences, Anesthesiology & Intensive Care Medicine, University Hospital, Uppsala University, Uppsala, SE-75185, Sweden

Received February 12, 2018; Accepted August 17, 2018

DOI: 10.3892/or.2018.6671

Abstract. The majority of modern treatment methods for malignant brain tumors are not sufficiently effective, with a median survival time varying between 9 and 14 months. Metastatic and invasive processes are the principal characteristics of malignant tumors. The most important pathogenic mechanism is epithelial-mesenchymal transition (EMT), which causes epithelial cells to become more mobile, and capable of invading the surrounding tissues and migrating to distant organs. Transforming growth factor-β1 (TGF-β1) serves a key role in EMT-inducing mechanisms. The current study presented the interaction between hematopoietic stem cells and glioblastoma cells stimulated by TGF-β1 *in vitro*. The materials for the study were hematopoietic progenitor cell antigen CD34+ hematopoietic stem cells (HSCs) and U87 glioblastoma cells. Cell culture methods, automated monitoring of cell-cell interactions, confocal laser microscopy, flow cytometry and electron microscopy were used. It was demonstrated that U87 cells have a complex communication system, including adhesive intercellular contacts, areas of interdigitation with dissolution of the cytoplasm, cell fusion, communication microtubes and microvesicles. TGF-β1 affected glioblastoma cells by modifying the cell shape and intensifying their exocrine function. HSCs migrated to glioblastoma cells, interacted with them and exchanged fluorescent tags. Stimulation of cancer cells with TGF-β1 weakened the ability of glioblastoma cells to attract HSCs and exchange a fluorescent tag. This process stimulated cancer cell proliferation, which is an indication of the ability of HSCs to 'switch' the proliferation and invasion processes in glioblastoma cells.

Correspondence to: Dr Igor Bryukhovetskiy, School of Biomedicine of The Far Eastern Federal University, 8 Sukhanova Street, Vladivostok 690091, Russia
E-mail: igbryukhovetskiy@gmail.com

Key words: glioblastoma, hematopoietic stem cells, transforming growth factor-β1, intercellular interaction

Introduction

The treatment of malignant brain tumors is one of the most complex areas of modern medicine. Upon completing all standard modern treatments, the median survival time of patients with glioblastoma is 1 year (1). Less than one-quarter of patients with metastatic brain tumors have an 8-12-month survival rate (2). Metastatic and invasive processes are the principal characteristics of malignant tumors (3). The low treatment success rate may be attributed to the use of outdated methods that have limited effects on these processes (4).

Invasive and metastatic processes are now known to be associated with cancer stem cells (CSCs) (5). A high dose of radiation does not guarantee an effective elimination of these cells in the tumor node. The heterogeneity and dynamic nature of the glioblastoma stem cell population, in combination with the selective permeability of the blood-brain barrier for medicinal substances, explain why currently available agents remain unable to successfully eliminate these cells (6). These cells are unaffected by the external environment and respond to stimuli by producing new and more resistant clones of neoplastic cells; therefore, a combination of existing therapeutic methods, including chemotherapy and radiotherapy, is required to control CSCs.

Biomedical cell products consisting of a complex of a cell line and an adjuvant represent a novel type of antitumor agent, and are being developed to address the problem of CSC

resistance to standard treatment. The most promising agent is a leukoconcentrate of receptor-type tyrosine-protein phosphatase C ($CD45)^+$ and hematopoietic progenitor cell antigen CD34 ($CD34)^+$ mononucleocytes, with a high content of hematopoietic stem cells (HSCs). This class of cells is known for having a high propensity to migrate towards CSCs (7). As the evidence demonstrates, these cells are able to reach CSCs and affect certain signaling pathways associated with proliferation and invasion (7). In previous research, it was reported that intercellular cooperation with HSCs involves the transmission of the cytoplasmic content into glioma and carcinoma cells, which has a pronounced inhibitory effect on tumor cell activity (8). This phenomenon may be used for the regulation of CSCs by inhibiting the mechanisms that determine their invasive abilities.

However, the aggressiveness of glioblastoma does not only depend on the degree of tumor cell differentiation; it also depends on their specific molecular phenotype, formed during coordinated intercellular interactions under the influence of clonal selection factors. The key pathogenic mechanism for the transformation of the molecular phenotype of tumor cells is epithelial-mesenchymal transition (EMT), in which epithelial cells lose their apical-basal polarity, the cytoskeleton is reorganized, components of the extracellular matrix are secreted, and the cells become more mobile and capable of invasion into the surrounding tissues and migration to distant organs (9-11). In relation to neuroepithelial tumors, this mechanism allows for the transformation of a primary glioma into a secondary glioblastoma, the transition from a proneural subtype of the tumor to a mesenchymal one, the creation of more aggressive clones of CSCs and the generation of new CSC populations (12).

Transforming growth factor (TGF)-β1 serves a key role in EMT-inducing mechanisms. This cytokine has been demonstrated to trigger EMT in certain cases of breast cancer (13), renal carcinoma (14), intestinal tumors (15-17), pancreatic cancer (18) and glioblastoma (19). Previous research (20) demonstrated that stimulation of U87 MG cell lines with TGF-β1 significantly increases the production of proteins associated with invasion, proliferation, migration, DNA regeneration, stemness, and resistance to drugs and radiation. The resulting pool of glioblastoma cells has a molecular phenotype that is very similar to that of CSCs (21). It was reported that in human glioblastoma tumor cells, only two signaling pathways (the integrin and focal adhesion pathways) are available for regulatory effects on gene expression processes in the CSC nucleus (20).

It is likely that the upregulation of the protein components of these signaling pathways due to EMT determines the interactions of the CSCs with the microenvironment and extracellular matrix. Theoretically, normal $CD45^+$ $CD34^+$ stem cells are able to regulate these processes during their interaction with CSCs, which may become a key point in cancer therapy and for overcoming therapeutic resistance. Bone marrow cells represent 30-50% of non-neoplastic glioblastoma cells. The aim of the present study was to investigate patterns of interaction between hematopoietic stem cells and glioblastoma cells stimulated by TGF-β1 *in vitro*.

Materials and methods

Cancer cells. The current study used human glioblastoma U-87 MG cells (American Type Culture Collection® HTB-14™; Manassas, VA, USA). This cell line is not the original U87 line established at the University of Uppsala (Uppsala, Sweden), although it is likely to be derived from a glioblastoma of unknown origin (21). However, as demonstrated in a previous study, cells of this line expressing the epitope prominin-1 (CD133) have high similarity of proteasomal profiles with neural $CD133^+$ human stem cells and significant proteomic differences compared with normal mesenchymal stem cells of the human bone marrow (20). In a previous study (19), stimulation of U87 glioblastoma cells with TGF-β1 led to a significant increase in the expression of proteins associated with EMT, which markedly increased their invasiveness. These arguments served as the basis for choosing this line of tumor cells for studying the processes of cell-cell interaction *in vitro*.

Human bone marrow cells. A leukoconcentrate of $CD45^+$ mononucleocytes mobilized from the peripheral blood following an injection of a granulocyte colony-stimulating factor (filgrastim) was used, according to a previously described method (22). The cells were provided freely by the CJSC NeuroVita Clinic of Restorative and Interventional Neurology and Therapy (Moscow, Russia), with the donors' permission. According to the supporting documents, the sample contained 4.5% cells with a $CD34^+CD45^+$ immunophenotype and 1.8% cells with integrin-$β1^+$, CD44 antigen ($CD44)^+$, 5'-nucleotidase$^+$ and Thy-1 membrane glycoprotein$^+$ markers. An immunosorting method was used for isolating $CD45^+$ $CD34^+$ cells from the leukoconcentrate (21), and these cells were used for the present study. The use of human samples in this study was approved by the Ethical Committee of the School of Biomedicine, The Far Eastern Federal University (Vladivostock, Russia; minute no. 1 of February 2nd 2017) and the Academic Council of the School of Biomedicine.

The cells were frozen and cultivated at 37˚C and 5% CO_2, in Dulbecco's modified Eagle's medium (DMEM; Gibco; Thermo Fisher Scientific, Inc., Waltham, MA, USA) with 10% fetal bovine serum (FBS; Gibco; Thermo Fisher Scientific, Inc.) and 10,000 U/ml penicillin/streptomycin, with 25 mg/ml fungizone. Cells were stained with fluorescent dyes and used for subsequent experiments.

Cell staining with fluorescent dyes. The cells were stained with CellTracker™ Red CMTPX Dye (cat. no. C34552; Molecular Probes; Thermo Fisher Scientific, Inc.; λ, 546 nm; 15 μM in DMEM; 25 min; 37˚C) and Vybrant® CFDA SE (cat. no. V12883; Molecular Probes; Thermo Fisher Scientific, Inc.; λ, 488 nm; 25 μM in PBS; 25 min; 37˚C), according to the manufacturer's protocols. Fluorescence was analyzed using a Carl Zeiss LSM 710 confocal laser-scanning microscope (Carl Zeiss AG, Oberkochen, Germany) with a standard set of filters. Lenses with magnification x10, x20 and x40 were used for observation.

Experimental design. The effects of recombinant human TGF-β1 (Sigma-Aldrich; Merck KGaA, Darmstadt, Germany) on glioblastoma cells were studied in 24-well plates; each well was seeded with $3x10^4$ cancer cells stained with CMTPX. TGF-1β, at a concentration of 10, 20 or 30 ng/ml, was placed into the culture medium, while the control wells contained cells without TGF-1β. The experiment was conducted with

the computer-aided Cell IQ system (CM Technologies GmbH, Elmshorn, Germany).

To study the migration of $CD45^+$ $CD34^+$ cells, 24-well plates with preset cell culture inserts were used, each with a pore size of 8 μm (SPL Life Sciences, Pocheon, Korea). The cell culture inserts were seeded with $3x10^4$ cancer cells stained with CMTPX dye; the wells contained $6x10^4$ HSCs stained with CFDA dye, and certain wells contained cultures with 10 ng/ml TGF-1β. In the control group, HSCs were also introduced into the wells, although the inserts had the culture medium without any cells or additives. Analysis was conducted with a flow cytofluorometer.

The process of exchanging a fluorescent tag was examined by co-culturing the cells at a ratio of 1:1, specifically $2.5x10^4$ cancer cells stained with red CMTPX with $2.5x10^4$ monocytes stained with green CFDA; certain wells contained 10 ng/ml TGF-1β. For monitoring, a confocal laser microscope was used for 96 h. Lenses with magnification x10, x20 and x40 were used for observation. The samples were placed in a chamber filled with 5% CO_2. Images were captured every 3 h. HSC adhesion to cancer cells was also studied using an electron microscope. Cells were cultured in DMEM with 10% FBS and 0.5% penicillin/streptomycin in Petri dishes for 72 h, following which the cells were extracted, washed and centrifuged, (120 x g; 5 min; 37˚C), fixed and embedded for further analysis.

To study the proteomes of the glioblastoma cells, a combination of high-performance liquid chromatography and mass spectrometry was used. The label-free method (21) was applied for evaluating the protein expression levels. The purposes of the study required the primary emphasis of the bioinformatic analysis to be placed on marker proteins of EMT and proteins of signaling pathways determining the interactions between cancer cells and the extracellular matrix.

Electron microscopy. The cells were fixed in 2.5% glutaraldehyde for 1 h, and washed in PBS twice (30 min/wash; 25˚C). Post-fixation was conducted in osmium for 1 h, following which the cells were dehydrated in 30, 50, 70 and 80% ethanol, and twice in 96% ethanol, for 10-15 min in each solution (25˚C). Subsequently, the samples were treated with ethanol-acetone at ratios of 3:1, 1:1 and 1:3 for 15 min in each solution (25˚C). The samples were embedded in resin (Epon-812, 4.4 ml; dodecenylsuccinic anhydride, 3.7 ml; methyl nadic anhydride, 1.9 ml) by infiltrating them into a graded series of acetone and resin mixture with a 3:1 ratio for 30 min, 1:1 for 2 h, 1:3 for 30 min, and resin alone for 12 h (25˚C). The embedding was finalized as follows: Two drops of accelerator per 1 ml of resin; and polymerization lasting for 72 h at 60˚C. Sections of 70-nm thickness were prepared using Ultracat E Reichert (Leica Microsystems, Inc., Buffalo Grove, IL, USA). The sections were stained with the following solutions: 1% uranyl acetate for 6 min; and lead citrate for 1.5 min. The transmission electron microscope (Libra 120; Carl Zeiss AG) was used for visualization of the results.

Flow cytofluorometry. The exchange of a fluorescent tag was additionally studied with a flow cytofluorometer. The cells stained with fluorescent tracers were extracted using trypsin and washed by double centrifuging in PBS (120 x g; 3 min; 37˚C). The precipitate was resuspended in 400 μl PBS, and analyzed with a BD Accuri® C6 flow cytometer (BD Biosciences, Franklin Lakes, NJ, USA). At least 10,000 single cells were analyzed in each sample. To distinguish single cells from aggregated ones, and to exclude the aggregated cells from the analysis, the following methods were used: A combination of signals from forward (value proportional to the size of the cells) and side (value characterizing the cell structure) light scattering; and the combination of the intensity of the peak signal against the intensity of integrated forward or side scattering signals. The results obtained were analyzed with Kaluza 1.3 software (Beckman Coulter, Inc., Brea, CA, USA).

Comparative analysis of cellular proteomes. Cancer cells (50,000) were seeded into 6-well plates and cultivated at 37˚C with 5% CO_2 to reach 30% confluence, in DMEM/F12 (Gibco; Thermo Fisher Scientific, Inc.) medium containing 10% FBS, 1% 200 mM L-glutamine and 20 mM HEPES. Subsequently, the cells were washed with Hanks' Balanced Salt Solution and transferred into DMEM/F12 serum-free medium with the addition of 5 ng/ml TGF-β1 for 72 h. The cells of the monolayer culture were extracted, the precipitate was centrifuged out (120 x g; 10 min; 25˚C), supernatant was removed, and the cells were resuspended in 3 ml PBS (pH 7.4). PBS washing was repeated twice. The cells were lysed with a Mammalian Cell Lysis kit (Sigma-Aldrich; Merck KGaA). The received samples were purified from low-molecular components using Agilent 5K MWCO Spin Concentrators for Proteins (Agilent Technologies GmbH, Waldbronn, Germany). Tryptic cleavage: Lysates were added to 2.2.2-trifluoroethanol (Reagent Plus; Sigma-Aldrich; Merck KGaA), NH_4HCO_3 (Ultra; Fluka Chemie AG, Buchs, Switzerland) and trichloroethylphosphate (Fluka Chemie AG) (1 h; 600˚C). Aqueous iodoacetomide (Sigma-Aldrich; Merck KGaA) was added (30 min; 250˚C); subsequently, NH_4HCO_3 solution, water and trypsin solution (porcine pancreatic; proteomics grade; demethylated; Sigma-Aldrich; Merck KGaA) in 1 mM hydrochloric acid (Purum; Chimmed, Moscow, Russia) (18 h; 370˚C). Solutions were analyzed by mass spectrometry for trypsinolysis completeness, which was controlled by the peaks of tryptic peptides and by the areas of peaks with m/z 842.51 Da and 421.76 Da. Mass-spectrometry: Tryptic peptides were analyzed in the nanoflow chromatograph Dionex Ultimate 3000 in combination with mass spectrometer LTQ Orbitrap XL (Thermo Fisher Scientific, Inc.) with a nanospray ionization ion source. Mass spectra were obtained using the positive ion mode in the m/z 300-2,000 Da range, a needle voltage of 1.7 kB, a source temperature of 200˚C, a voltage to capillary of 43 B, and to lens 165 B. Mass spectra were registered in the orbital trap in Fourier transform mode; tandem spectra were obtained by ionization induced by collisions in a linear trap (enhanced scanning mode).

To identify proteins, the mass spectra were converted into. mgf files using Proteome Discoverer 1.0 software (Thermo Fisher Scientific, Inc.); pattern WF_Spectrum_Export_MGF was set as the default except for the mass range (between 300 and 10,000 Da) and retention time (0-180 min). Protein searches were performed on the local server with Mascot

Server 2.3.02 software (Matrix Science, Ltd., London, UK). Search parameter were as follows: Database, National Center for Biotechnology Information non-redundant GenBank (version, January 25th 2012); species, *Homo sapiens*; enzyme, trypsin; number of missed cleavages, 2; accuracy of parent ion mass, 10 ppm; fragments, 0.8 Da; ion trap. Identified proteins were sorted by MudPIT score (Mascot Server 2.3.02 software; Matrix Science, Ltd.; http://www.matrixscience.com/server.html), presenting peptides at a significance level of $P<0.05$. Received lists of identified proteins and mass spectra were uploaded to Skyline 1.2.0.3303 (University of Washington, Seattle, WA, USA; https://skyline.gs.washington.edu/labkey/project/home/software/Skyline), and peak peptide areas were received for every probe. The areas of all the peaks of every identified peptide were summed and normalized according to total area of all identified peaks in the probe. Biological processes, molecular functions, cellular localization and protein signaling pathways were annotated using the PubMed (https://www.ncbi.nlm.nih.gov/pubmed), PANTHER (http://www.pantherdb.org), Gene Ontology (http://geneontology.org) and Kyoto Encyclopedia of Genes and Genomes databases (https://www.genome.jp/kegg/kegg1.html).

Statistical analysis. The data were processed using GraphPad Prism 4.0 software (GraphPad Software, Inc., La Jolla, CA, USA). Results of the migration and electron microscopy study are presented as boxplots, indicating quartiles 1 and 3, the median, and the minimum and maximum data values (whiskers). Statistical analysis was performed using the Mann-Whitney U test. The results were considered to be statistically significant at $U<U_{crit}=93$ ($n=19$) for $\alpha=0.01$; and $U<Ucrit=113$ ($n=19$) for $\alpha=0.05$.

The results of the study of the effects of TGF-β1 on glioblastoma cells are presented as the mean ± standard error of the mean. The analysis of variance F-test was used for data analysis ($n=75$; $m=25$) followed by a post hoc t-test with Bonferroni correction. Results were considered to be statistically significant at values of family-wise error rate $<P<\alpha$.

Results

Stimulation of control cells with TGF-β1. TGF-β1 (30 ng/ml) did not have a pronounced effect on the proliferation of U87 glioblastoma cells. The gradual reduction of the TGF-β1 concentration to 20 and 10 ng/ml (Fig. 1) slowed the cell proliferation and led to notable morphological alterations (Fig. 2A and B). Glioblastoma cells were dispersed over the surface of the well and created conglomerates with an evenly distributed fluorescent tag. These were connected with the microtubes of dispersed cells, which was particularly noticeable in the panoramic view (Fig. 2C and D). This phenomenon was absent in the control group.

The analysis of electronograms revealed cells with large nuclei and irregular shapes, dispersed chromatin and well-defined nucleoli. The cytoplasm of the control cells contained larger areas of lower electron density and dispersed distribution of components resembling carbohydrate inclusions, among which there were round objects resembling lipid droplets (Fig. 3A). Touching the cell surface, they created adhesion and contact bands with a spongy amorphous matrix spread among them (Fig. 3B). In places, there were large areas of cell adhesion with interdigitation represented by adjacent cellular membranes that had their surface dissolved in sections, thus creating zones of cytoplasmic fusion with homogenous content (Fig. 3C). The scanning microscopy revealed certain cells with fused membranes (Fig. 3D), and cells joined by cytoplasm tube-like extensions that allowed single cells (Fig. 3E) and cell conglomerates (Fig. 3F) to interact with each other. Stimulation of glioblastoma cells with TGF-β1 was accompanied by a decrease in the number of intercellular contacts and the almost complete disappearance of specific inclusions in the cytoplasm (Fig. 4). The presence of numerous filopodia indicated an increased rate of cancer cell mobility.

Interaction of HSCs and cancer cells in vitro. According to the automated monitoring, the migration of HSCs to the inserts with glioblastoma cells in the non-stimulated experimental group was more dynamic compared with the group stimulated with TGF-β1 (Fig. 5). According to the monitoring data, the increase in the number of HSCs migrating to U87 cells enhanced the ability of the tumor cells to detach from the substrate and move across the well surface.

After 48 h, cancer cells in the control group and the experimental co-culture with adhesive HSCs were arranged in grape-like clusters (Fig. 6). After 12 h, in addition to the fluorescent cells stained with CMTPX RED (λ, 546 nm; red tag) and adherent HSCs stained with CFDA (λ, 488 nm; green tag), green fluorescent objects of a smaller size began to appear on the surface of and inside glioblastoma cells (Fig. 7). This phenomenon was also present in the cell culture stimulated by TGF-β1; however, by the end of the experiment there were notably fewer HSCs in the well with co-culture compared with the control group.

The exchange of the fluorescent tag was not one-sided. As the observation progressed, the fluorescence of the stem cells adherent to glioblastoma cells exhibited dominant yellow tones (Fig. 7) that were attributed to a spectral intersection of fluorescent signals from CFDA (λ, 488 nm) and CMTPX Red (λ, 546 nm) dyes. This was likely to have been caused by the fluorescent tag carried by the cancer cells. In the non-stimulated group these results were similar. Interaction with HSCs had a pronounced effect on glioblastoma cells, which was indicated by the proliferation rate returning to a level similar to that of the control group (Fig. 8).

Comparative analysis of cancer cell proteomes. This phase of the experiment involved analyzing the impact of TGF-β1 on the molecular phenotype of glioblastoma cells. During the incubation of the U87 line cells in the medium with TGF-β1, 637 proteins exhibited a significant alteration in expression; 513 proteins had an increase in expression, while 124 proteins had an expression decrease ($P<0.01$). Bioinformatics analysis of proteins with significant alterations in their expression was based on their status as EMT markers (Table I) and their involvement in signaling mechanisms regulating cellular interactions with the microsurroundings and extracellular matrix (Table II). Fig. 9 presents a schematic representation of protein upregulation under the influence of TGF-β1. These proteins are components of the interaction between the extracellular matrix and the cell membrane. There are also a

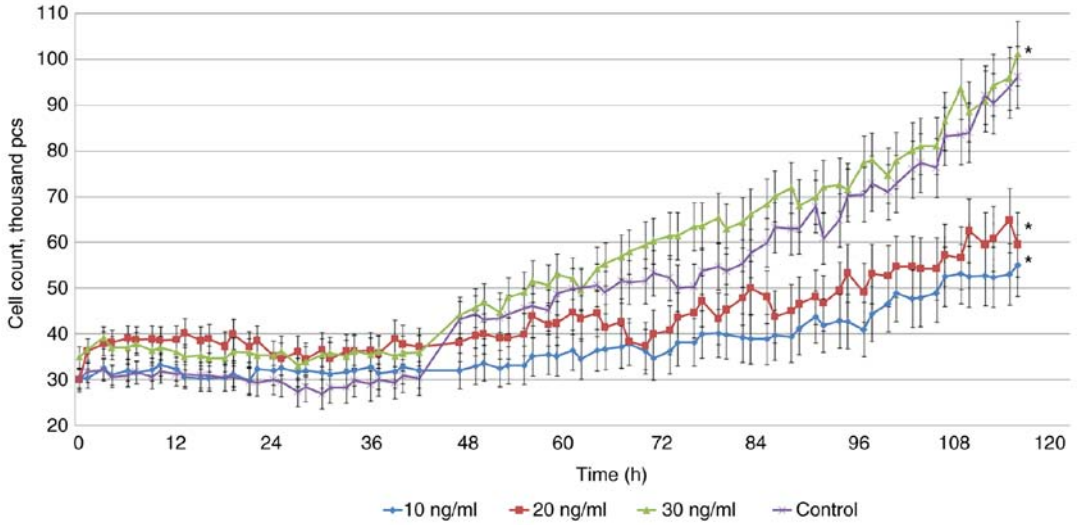

Figure 1. Growth dynamics of glioblastoma U87 cells treated with transforming growth factor-β1. *Family-wise error rate <P=0.01 <α=0.05/4 vs. control.

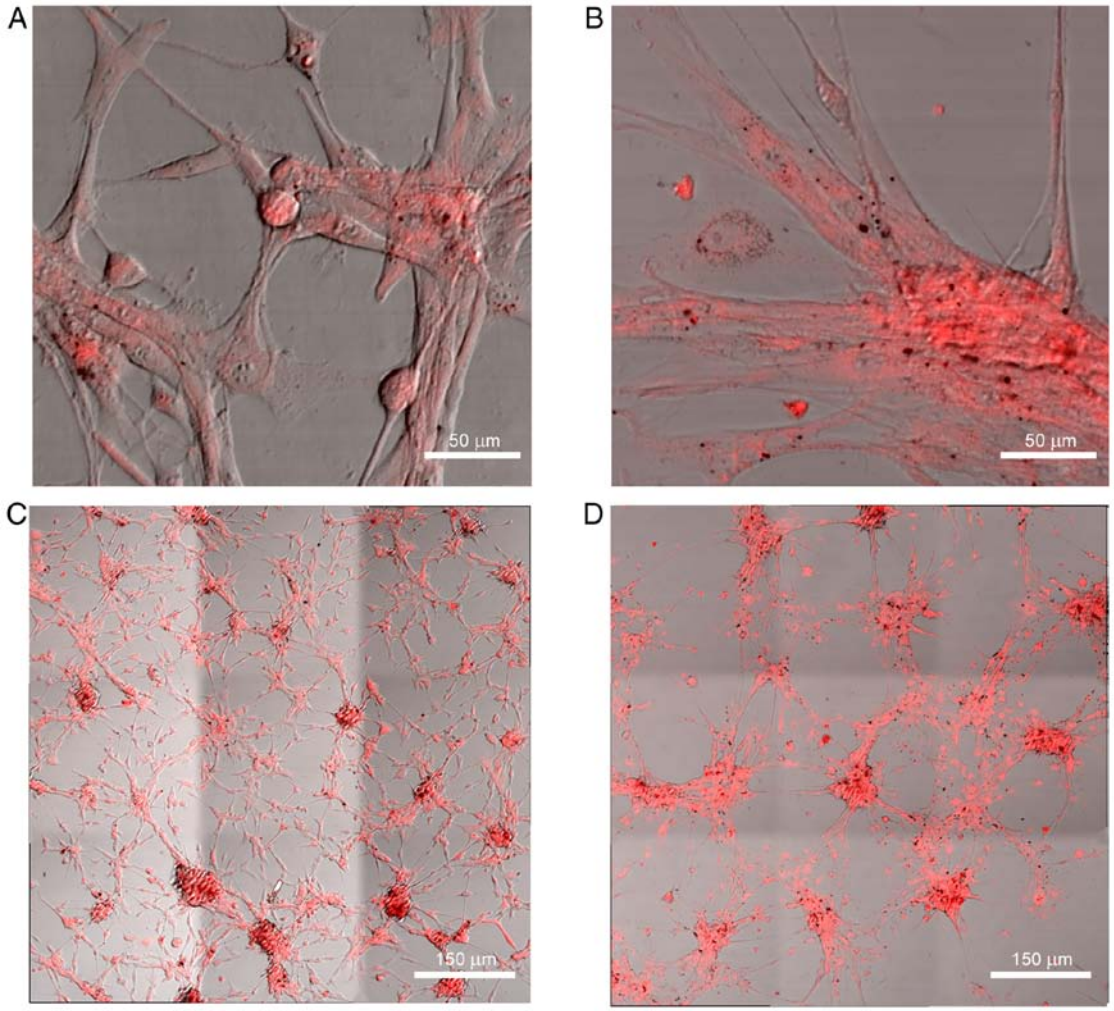

Figure 2. Morphological features of cancer cells treated with TGF-β1. Cancer cells were stained with CellTracker™ Red CMTPX. The images were captured following 72 h of treatment. (A) Glioblastoma U87 cells (control group); (B) glioblastoma U87 cells treated with 10 ng/ml TGF-β1; (C) panoramic view of nine slides of control U87 cells; (D) panoramic view of nine slides of U87 cells treated with 10 ng/ml TGF-β1. TGF-β1, transforming growth factor-β1.

number of proteins that are simultaneously adjusted with the components of the ECM in this schematic. The synthesized components of the extracellular matrix allow cells to invade surrounding tissues. The components of the integrin signaling

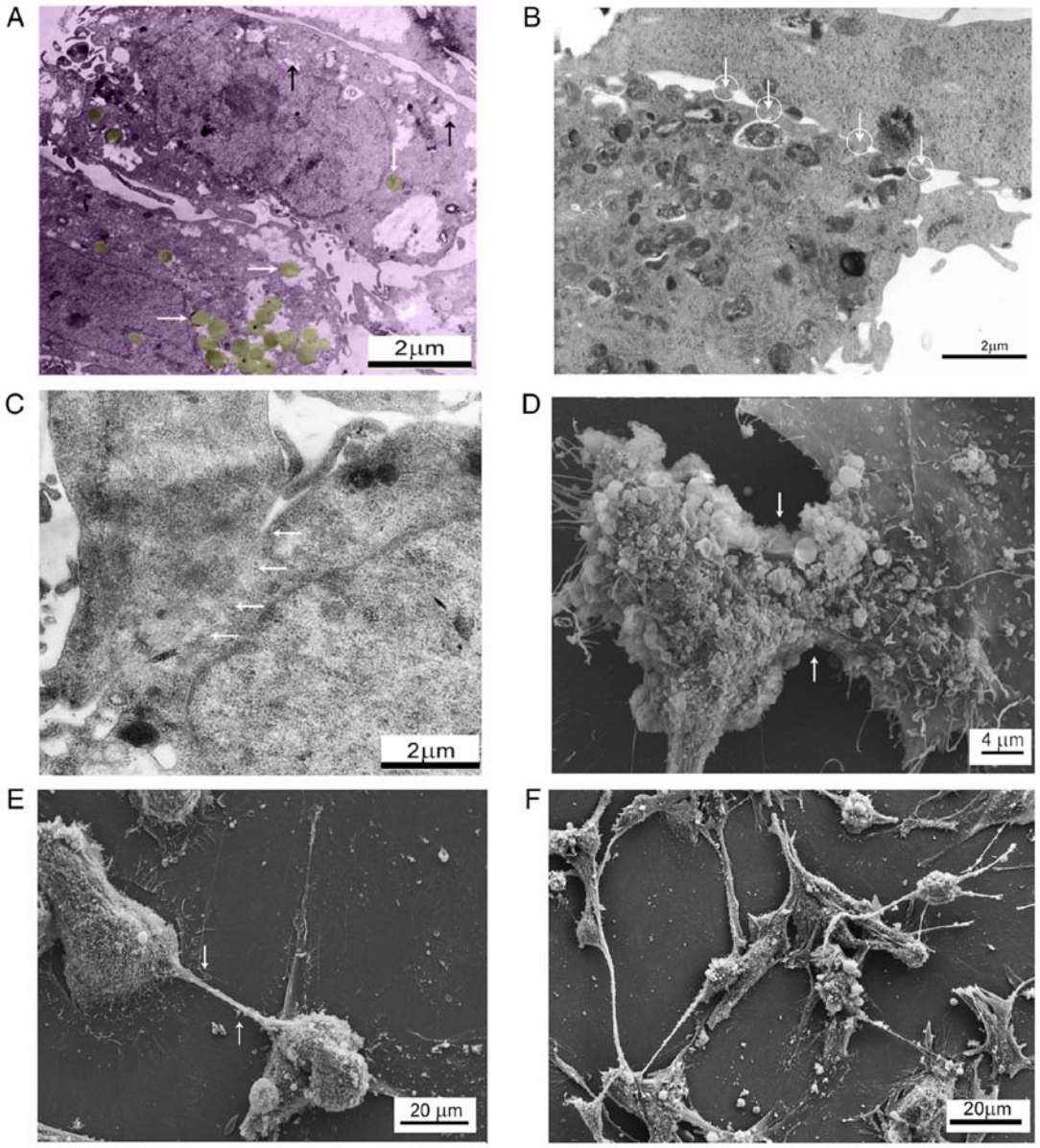

Figure 3. Microphotographs of glioblastoma U87 cells. (A) Carbohydrate inclusions and lipid droplets in a glioblastoma cell. (B) Adhesive contacts between glioblastoma cells; (C) extensive merger of glioblastoma cells, (D) partial cytoplasmic fusion between glioblastoma cells. (E) Cytoplasmic bridge connecting the glioblastoma cells. (F) Conglomerate of glioblastoma cells connected by cytoplasmic extensions.

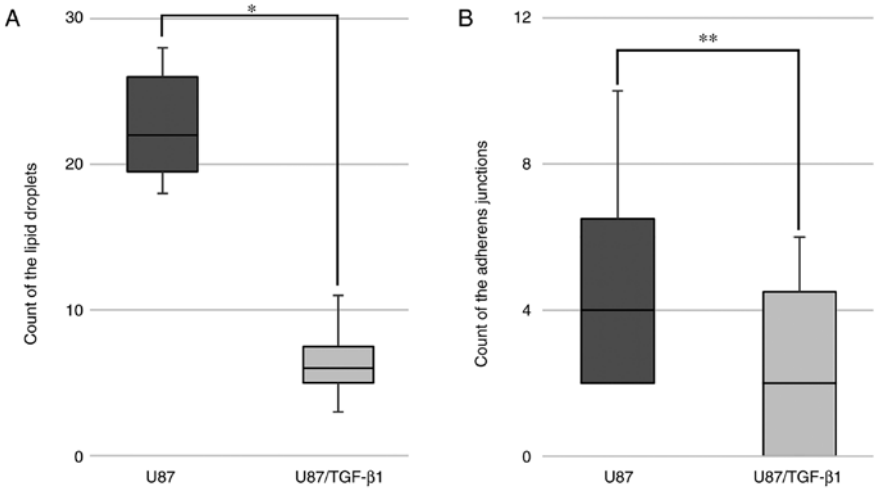

Figure 4. Effect of TGF-1β on glioblastoma cells. (A) Quantity of carbohydrate inclusions and lipid droplets. (B) Number of contacts between glioblastoma cells. *P<0.01, **P<0.05. TGF-β1, transforming growth factor-β1.

Table I. Alteration in the expression of proteins involved in epithelial-mesenchymal transition in cells of the U87 human glioblastoma line, following stimulation with TGF-β1.

Abbreviation	Protein name	Ratio, TGF-β1/control
CDH1	E-cadherin	↓
OCLN	Occludin	↓
CLDN1	Claudin1	0.65
VIM	Vimentin	2.81
FN1	Fibronektin1	4.10
FNDC3B	Fibronectin type III domain containing 3B	3.32
Actl6a	Actin-like 6A	↑
Actn1	Actinin, α1	2.04
ARPC3	Actin related protein 2/3 complex subunit 3	2.31
MYBPC3	Myosin binding protein C, cardiac	5.71
Myo1C	Myosin IC	2.82
MYO5A	Myosin VA (heavy chain 12, myoxin)	↑
Myo7a	Myosin VIIA	↑
MMP2	Matrix metallopeptidase 2	2.85
MMP9	Matrix metallopeptidase 9	2.10
MMP14	Matrix metallopeptidase 14	↑
ADAMTS1	ADAM metallopeptidase with thrombospondin type 1 motif, 1	↑

[a]Arrows indicate proteins whose expression was completely abrogated (↓) or which appeared for the first time (↑) following stimulation with TGF-β1. TGF-β1, transforming growth factor-β1.

Table II. Proteins of the integrin and focal adhesion signaling pathways with enhanced expression in glioblastoma cells of the U87 line after stimulation of TGF-β1.

Abbreviation	Protein name	Ratio, TGF-β1/control
ITGA2	Integrin, α2	1.91
ITGA8	Integrin, α8	↑[a]
ITGAX	Integrin, αX	1.61
ITGA3	Integrin, α3	0.81
ITGAV	Integrin, αV	1.51
ITGA5	Integrin, α5	1.55
ITGB2	Integrin, β2	1.21
ITGB3	Integrin, β3	2.01
ITGB1	Integrin, β1	1.52
Memo1	Mediator of cell motility 1	↑
LAMB1	Laminin, β1	7.22
Col15a1	Collagen, type XV, α1	2.42
COL1A2	Collagen, type I, α2	3.59
COL6A1	Collagen, type VI, α1	2.34
COL7A1	Collagen, type VII, α1	4.58
RHAMM	Hyaluronan-mediated motility receptor	↑
CDC42	Cdc42 GTPase-activating protein	↑
RhoA	Ras homolog gene family, member A	1.45
RHOC	Ras homolog gene family, member C	1.21
ROCK2	Rho-associated, coiled-coil containing protein kinase 2	1.38
CK2A2	Casein kinase 2, alpha prime polypeptide	2.61
CTNND1	Catenin (cadherin-associated protein), δ1	2.60
Cul1	Cullin 1	2.53
DAAM1	Dishevelled associated activator of morphogenesis 1	6.54
APC	Adenomatous poliposis coli	↑

[a]Arrows (↑) indicate proteins that were not present in the control group and appeared for the first time following stimulation with TGF-β1. TGF-β1, transforming growth factor-β1.

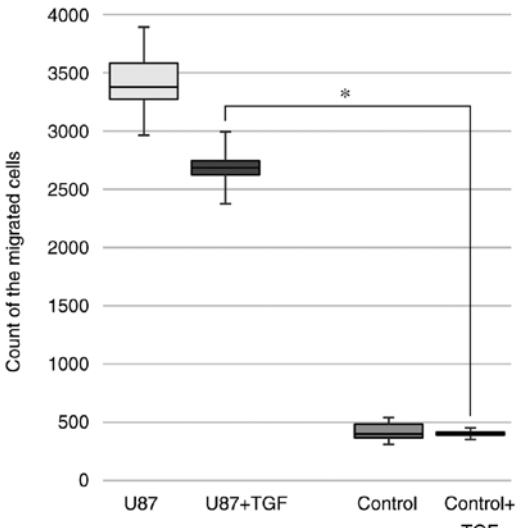

Figure 5. Effect of TGF-β1 on hematopoietic stem cell migration to glioblastoma cells. *P<0.01. TGF-β1, transforming growth factor-β1.

pathway, following stimulation with TGF-β1, also undergo upregulation, which transforms cells stimulated by TGF-β1 into cancer stem cells (Table II; Fig. 9)

Discussion

The role of TGF-β1 in the process of carcinogenesis of glioblastoma multiforme is extremely complex. According to a previous study, when TGF-β1 functions under normal conditions it inhibits cell proliferation, arrests the cell cycle, and initiates differentiation or apoptosis (22). Following neoplastic transformation, certain parts of the TGF-β1 signaling pathway are altered, and TGF-β1 no longer exerts its effects on the cell (22). This may explain the present observation of high proliferation rates in glioblastoma cells treated with 30 ng/mg TGF-β1. A high concentration of TGF-β1 may be essential for neoplastic growth. In normal *in vivo* conditions, TGF-β1 arises from the cancer cells themselves, fibroblasts, cells of cancerous microglia/macrophages, and possibly from immunocytes recruited by the tumor (22).

It is likely that the intensive growth of cancer cells creates competition for oxygen and other sources of nutrition, which leads to inhibition of cell metabolism and a lower level of TGF-β1 synthesis. Therefore, this transformation may initiate cell migration from hypoxic areas to other areas with a better blood supply, where the local microenvironment may be more favorable. This hypothesis is supported by the gradual decrease in replicative activity among cancer cells in the present study,

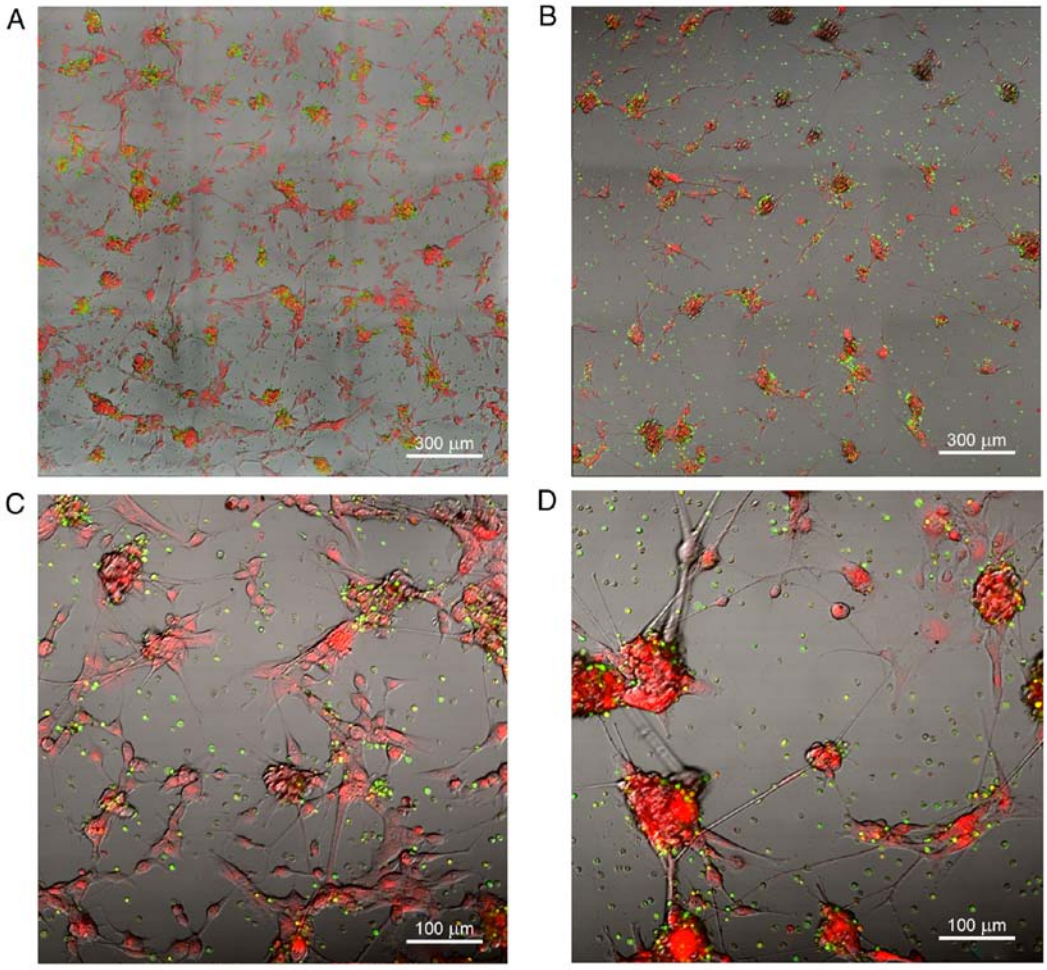

Figure 6. Morphological features of glioblastoma cells in co-culture with HSCs 72 h after the start of the experiment. Cancer cells were stained with Red CMTPX and HSCs were stained with CFDA SE. (A) U87 glioblastoma cells in co-culture with HSCs (panoramic view of nine slides); (B) U87 glioblastoma cells in co-culture with HSCs following treatment with 10 ng/ml TGF-β1 (panoramic view of nine slides); (C) U87 cells co-cultured with HSCs; (D) co-culture treated with 10 ng/ml TGF-β1. HSC, hematopoietic stem cell; TGF-β1, transforming growth factor-β1.

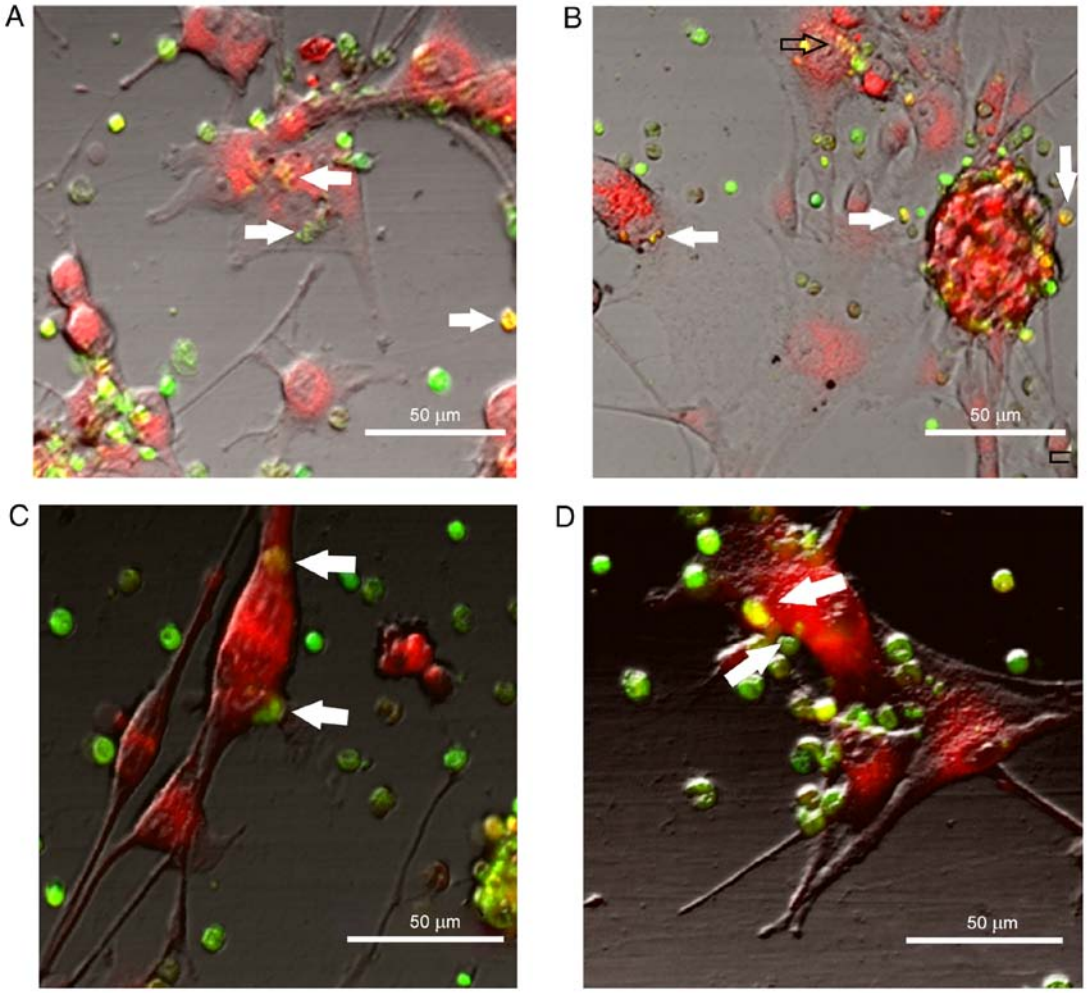

Figure 7. Exchange of a fluorescent tag between HSCs and cancer cells 72 h after the start of the experiment. Cancer cells were stained with Red CMTPX and HSCs were stained with CFDA SE. (A) Fluorescent tag exchange between HSCs and U87 glioblastoma cells. (B) Exchange of a fluorescent tag between HSCs and U87 cancer cells after treatment with 10 ng/ml of TGF-β1. (C) Fusion or phagocytosis of HSCs and U87 glioblastoma cells. (D) Fusion or phagocytosis of HSCs and U87 glioblastoma cells following treatment with 10 ng/ml of TGF-β1. Arrows indicate the cells involved in fluorescent tag exchange. HSC, hematopoietic stem cell; TGF-β1, transforming growth factor-β1.

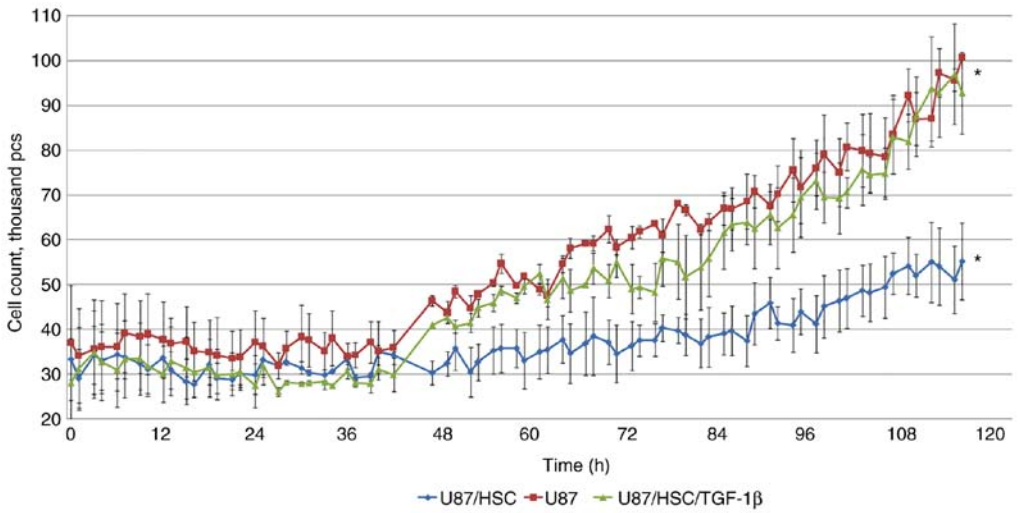

Figure 8. Effect of TGF-β1 on the growth dynamics of glioblastoma U87 cells in co-culture with HSCs. *Family-wise error rate <P=0.01 <α=0.05/3 vs. U87. TGF-β1, transforming growth factor-β1.

when the TGF-β1 concentration was reduced to 20 and 10 ng/ml. Other studies also support this hypothesis (18,19).

On the one hand, this mechanism hinders the progress of the neoplastic process; on the other hand, it ensures the

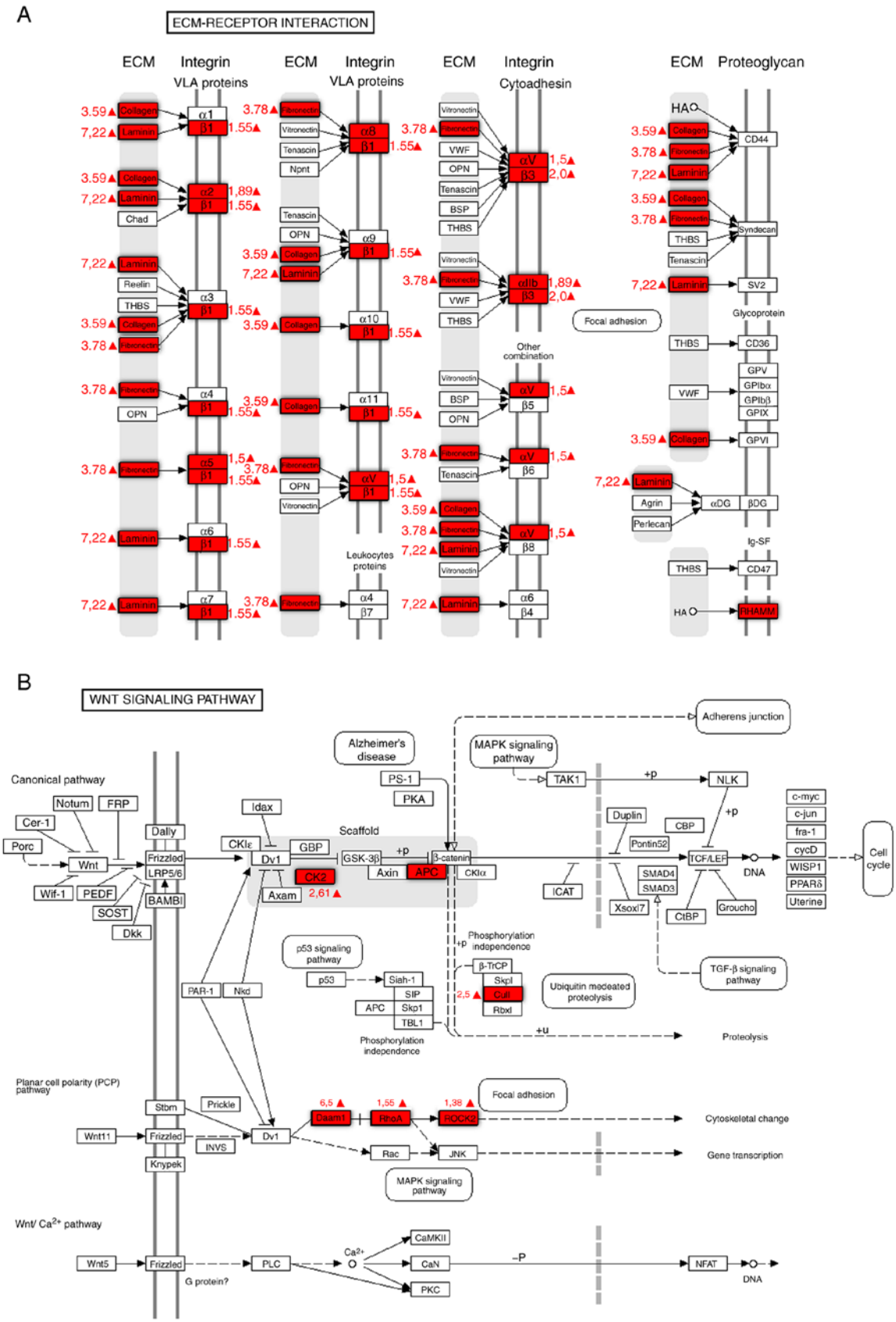

Figure 9. ECM-receptor interactions and WNT signaling pathways. Maps of (A) ECM-receptor interactions and (B) WNT signaling pathways are presented. Proteins with increased expression in glioblastoma cells treated with transforming growth factor-β1 are highlighted in red. ECM, extracellular matrix.

selection of hypoxia-resistant cellular elements that make a tumor more aggressive. Switching from a proliferation to a migration program is reflected by more active interaction with the surface of the culture plate. TGF-β1 stimulation leads to

an intensification of exocrine function in cancer cells, causing a decrease in the number of intracellular inclusions and intercellular contacts, and creating multiple exocyte bubbles and actively releasing cell contents (22). The synthesis of extracellular matrix components combined with the production of proteolytic enzymes is an important part of a complex invasive growth program (23). By secreting components of the extracellular matrix and interacting with them, a cancer cell may penetrate the surrounding tissues. The ability of cancer cells to synthesize components of the extracellular matrix may be considered to be a crucial mechanism in shaping the aggressive nature of cancer (24). The production of matrix proteins and molecules involved with cellular adhesion and migration explains the marked alteration in the shape of cells and the appearance of multiple filopodia (25).

However, the present study suggested that these changes do not exclude a possibility of coordinated interaction among glioblastoma cells due to a complex system of intercellular communication creating a unified system of cells.

Cross-talk between cells in living organisms is based on the exchange of information. With the help of intercellular interactions, the coordinated regulation of metabolism, differentiation and cell proliferation occurs in different tissues. The complex system of microtubes joining glioblastoma cells merits consideration. Certain studies have suggested that there is a cancer cell communication network (24-27). This network is thought to be responsible for transporting proteins that confer chemoresistance and radiation resistance, proteins responsible for DNA repair, microRNAs (miRNAs) disrupting the processes of epigenetic control over oncogene expression, the hierarchical development of glioblastoma cells (6), and the creation of CSC niches (21).

It is known that the development of an invasive phenotype in cancer cells following stimulation by TGF-β1, as described by the authors of the present study (20) and others (23), is not limited by their localization. Appearing as a response to the local conditions, a transformed resistant and invasive molecular phenotype is transmitted to other cells through adhesive contacts, multiple connective tubes, the fusion of cancer cells and the production of microvesicles. To an extent, this system of communication may explain the dynamic nature of CSC populations, and the presence of cancer/stem progenitor cells, tumor-inducing cells and other neoplastic elements with properties that are not typical for ordinary glioblastoma cells (6,13,14).

The production of microvesicles is one of the less-studied types of communication between neoplastic cancer cells (24-26). This type of communication is used for long-distance transportation of materials or to protect materials from an aggressive microenvironment. In addition to DNA and RNA, microvesicles may transport CD44, $CD133^+$ mitogen activated protein kinase, epidermal growth factor vIII receptor, disintegrin and metalloproteinase domain-containing protein 10, Annexin A2 and certain pro-metastatic molecules (28-30). It is possible to transfer drug resistance between invasive glioma cells through exosomes (31). Therefore, it is possible make a justified assumption that microvesicle synthesis is a self-sufficient mechanism of tumor aggression, which renders it possible to transfer an invasive phenotype to other cells and tissues.

Normal $CD45^+$ $CD34^+$ HSCs are able to migrate to cells of different types, although they have increased mobility towards cancer cells. In animals with implanted glial brain tumors, intravenously injected HSCs migrate to the tumor nidus and accumulate in areas of invasion and necrosis (32). A previous study reported that hematopoietic $CD34^+$ $CD45^+$ stem cells migrate towards glioblastoma cells and interact with them, indicative of a strong association between these cell types (32). It is possible that by recruiting bone marrow cells, the tumor creates its own microenvironment, allowing it to optimize resources and escape the innate immune system and other defense mechanisms of the body (32). As demonstrated by fluorescent microscopy, HSCs attach themselves to cancer cells in 'piggy-back fashion', as described by Aboody *et al* (7). The method of electron microscopy failed to reveal specific intercellular contacts between the mononuclear cells and cancer cells. This may be associated with the disappearance of mononuclear cells, caused by the toxic products of glioblastoma cellular metabolism.

According to the results of the present study, TGF-β1 stimulation did not reduce the ability of glioblastoma cells to attract HSCs. The cells actively attached themselves to glioblastoma cells and exchanged fluorescent tags.

Exchanging a fluorescent tag during the interaction of normal stem cells and cancer cells suggests the possibility of transferring cellular proteins and other cytoplasm components that the dye adheres to. The results of the flow cytometry indicated the presence of cancer cells with a double fluorescent tag, which represented cells with new properties. It is noteworthy that the exchange of a fluorescent tag goes in both directions. The most likely mechanisms of these interactions are gap junction contacts, the exchange of biological information through microvesicles or the direct receipt of biological material secreted by the membrane of neoplastic cells (31).

Gap junction contacts (33) do not allow for the transfer of large protein molecules between cells, although they do allow cells to exchange miRNAs. Previously, miRNAs that inhibit [the Let-7 family, miRNA (miR)34, miR31, miR451, miR145, miR200/141, the miR14/15 family, miR23b, miR223 and miR224] (34) and stimulate (the miR17-92 cluster, miR21, H19, MALAT and HOTAIR/miR-10b) cellular transition to a pro-tumor phenotype have been described (35-37,28). Together with cellular proteins, these miRNAs may be transported to cancerous and non-cancerous cells through microvesicles, or may be transferred during cell fusion or contact. However, the possibility of direct absorption by non-cancer cells may not be ignored, and was partially demonstrated by the results of the fluorescence microscopy in the present study.

It is notable that during cell interactions, the proliferation speed of glioblastoma cells that were treated with TGF-β1 became similar to that of the control group. The intensified proliferation rates of glioblastoma cells stimulated by TGF-β1 while interacting with HSCs indicated the ability of normal $CD45^+$ $CD34^+$ stem cells to switch proliferation and migration programs, which is likely to be a focal point of HSC anti-tumor potential. This has significant theoretical importance. The triggering of EMT stimulates invasion and migration, accompanied by intensified interaction with the extracellular matrix and a decreased rate of cancer cell replication (13). The decline in replication activity to the control values suggested

a decreasing interaction with the extracellular matrix and an inhibition of invasion. In this respect, it may be proposed that the combination of a stem cell-based medication with cytostatic chemotherapy and radiation may be essential for the destruction of neoplastic cells.

However, the present experimental data are not sufficient for the successful implementation of cellular technologies in practice. It is necessary to have a clear understanding of what specific molecular mechanisms are activated in glioblastoma cell TGF-β1 stimulation, and how exactly HSCs are able to regulate them. The answers to these questions are not trivial. TGF-β1 stimulation of cancer cells is accompanied by substantial modification of their molecular phenotype, rendering them similar to cancer stem cells.

The integrin and focal adhesion signaling pathways are the most accessible pathways for regulatory influence in normal neural stem cells and stem cells of the bone marrow, and in cancer stem cells of human glioblastoma. The present study demonstrated that TGF-β1 stimulation of cancer cells was accompanied by a significant alteration in E-cadherin, occluding and claudin-1 production, and intensified synthesis of vimentin, actin and other EMT markers. However, the maximum upregulation was achieved for proteins of integrin and focal adhesion signaling pathways. This was not unexpected; increased expression of proteins regulating the interaction of cancer cells with the extracellular matrix during EMT is a logical outcome of TGF- β1 stimulation.

The fact that the focal adhesion proteins with increased expression (Ras homolog gene family, member A, Ras homolog gene family, member C, Rho-associated, coiled-coil containing protein kinase 2, dishevelled associated activator of morphogenesis 1 and cullin 1) were components of the WNT signaling pathway was noteworthy. Key components of canonical WNT/β-catenin pathway (CK2A2 and APC) appeared *de novo* as a reaction to stimulation. This signaling pathway is a strategically significant mechanism of stemness, indicating a possibility of developing CSC properties in these cells in response to invasion programs. Proliferation intensification in cancer cells with EMT upon interacting with HSCs indicates the ability of normal stem cells to regulate this process, and requires further study.

The following conclusions may be drawn from the present study. U87 glioblastoma cells have a complex system of communication, including adhesive intercellular contacts, areas of interdigitation with dissolution of the cytoplasm, cell fusion, communication microtubes and microvesicles. The effect of TGF-β1 on glioblastoma cell proliferation was inversely proportional to its concentration in the medium. When the concentration of TGF-β1 reached 10 ng/ml, it resulted in the modification of cell shape and the intensification of exocrine functioning. HSCs migrated to glioblastoma cells, interacted with them and exchanged fluorescent tags. Stimulation of cancer cells with 10 ng/ml TGF-β1 weakened their ability to attract HSCs and exchange a fluorescent tag. The proliferation rate of glioblastoma cells treated with TGF-β1 increased during intercellular interactions. TGF-β1 triggered the mechanisms of EMT in glioblastoma cells, which was accompanied by an alteration in the production of E-cadherin, occluding and claudin-1, and enhanced synthesis of vimentin and actin. Upregulation of the proteins of the integrin and focal adhesion signaling pathways was accompanied by an increase in the expression of proteins of the WNT signaling pathway. These processes indicated a direct association between the initiation of EMT and the stemness of the cancer cells phenotype. It is apparent that HSCs may be able to regulate this process, which requires continued research.

Acknowledgements

Not applicable.

Funding

The present study was funded by the Ministry of Education and Science of the Russian Federation (grant no. 14.584.21.0027; ID, RFMEFI58417X0027).

Availability of data and materials

The datasets used and/or analyzed during the current study are available from the corresponding author on reasonable request.

Authors' contributions

EM was involved in the experiments stimulating control cells with TGF-β1, and the interactions between HSCs and cancer cells *in vitro*, in addition to working on the text of the article. IB worked on the text of the article, proposed the study idea, developed the design, offered methodological support, organized the scientific team and provided scientific guidance on the experimental part of the study. AP undertook experiments on the interactions between HSCs and cancer cells *in vitro*. MK conducted the flow cytofluorometry. IL performed the work with the CellIQ system. YZ worked on the bioinformatics experiments and the text of the article. SZ performed the statistical analysis. PM performed experiments stimulating control cells with TGF-β1. ME conducted the electron microscopy. YK was involved in the experimental design and proteomic analysis, and worked on the text of the article. VS performed the proteomic analysis. HS consulted on the neuropathology aspects of this work, and worked on the text of the article. All authors read and approved the final manuscript.

Ethics approval and consent to participate

The use of human samples for this study was approved by the Ethical Committee of the School of Biomedicine, The Far Eastern Federal University (Vladivostock, Russia; minute no. 1 of February 2nd 2017) and the Academic Council of the School of Biomedicine. Consent was received.

Patient consent for publication

Not applicable.

Competing interests

The authors declare that they have no competing interests.

References

1. Torre LA, Bray F, Siegel RL, Ferlay J, Lortet-Tieulent J and Jemal A: Global cancer statistics, 2012. CA Cancer J Clin 65: 87-108, 2015.
2. Omuro A and DeAngelis LM: Glioblastoma and other malignant gliomas: A clinical review. JAMA 310: 1842-1850, 2013.
3. Hambardzumyan D and Bergers G: Glioblastoma: Defining tumor niches. Trends Cancer 1: 252-265, 2015.
4. Stupp R, Toms SA and Kesari S: Treatment for patients with newly diagnosed glioblastoma-reply. JAMA 315: 2348-2349, 2016.
5. Brown DV, Daniel PM, D'Abaco GM, Gogos A, Ng W, Morokoff AP and Mantamadiotis T: Coexpression analysis of CD133 and CD44 identifies proneural and mesenchymal subtypes of glioblastoma multiforme. Oncotarget 6: 6267-6280, 2015.
6. Bradshaw A, Wickremsekera A, Tan ST, Peng L, Davis PF and Itinteang T: Cancer stem cell hierarchy in glioblastoma multiforme. Front Surg 3: 21, 2016.
7. Aboody KS, Brown A, Rainov NG, Bower KA, Liu S, Yang W, Small JE, Herrlinger U, Ourednik V, Black PM, *et al*: Neural stem cells display extensive tropism for pathology in adult brain: Evidence from intracranial gliomas. Proc Natl Acad Sci USA 97: 12846-12851, 2000.
8. Bryukhovetskiy I, Bryukhovetskiy A, Khotimchenko Y and Mischenko P: Novel cellular and post-genomic technologies in the treatment of glioblastoma multiforme (Review). Oncol Rep 35: 639-648, 2016.
9. Garber K: Epithelial-to-mesenchymal transition is important to metastasis, but questions remain. J Natl Cancer Inst 100: 232-239, 2008.
10. Weng J, Zhang H, Wang C, Liang J, Chen G, Li W, Tang H and Hou J: miR-373-3p targets DKK1 to promote EMT-induced metastasis via the Wnt/β-catenin pathway in tongue squamous cell carcinoma. Biomed Res Int 2017: 6010926, 2017.
11. Xu H, Huang S, Zhu X, Zhang W and Zhang X: FOXK1 promotes glioblastoma proliferation and metastasis through activation of Snail transcription. Exp Ther Med 15: 3108-3116, 2018.
12. de Almeida Sassi F, Lunardi Brunetto A, Schwartsmann G, Roesler R and Abujamra AL: Glioma revisited: From neurogenesis and cancer stem cells to the epigenetic regulation of the niche. J Oncol 2012: 537861, 2012.
13. Morel AP, Lièvre M, Thomas C, Hinkal G, Ansieau S and Puisieux A: Generation of breast cancer stem cells through epithelial-mesenchymal transition. PLoS One 3: e2888, 2008.
14. Zhang N, Hong B, Zhou C, Du X, Chen S, Deng X, Duoerkun S, Li Q, Yang Y and Gong K: Cobalt chloride-induced hypoxia induces epithelial-mesenchymal transition in renal carcinoma cell lines. Ann Clin Lab Sci 47: 40-46, 2017.
15. Yang SW, Zhang ZG, Hao YX, Zhao YL, Qian F, Shi Y, Li PA, Liu CY and Yu PW: HIF-1α induces the epithelial-mesenchymal transition in gastric cancer stem cells through the Snail pathway. Oncotarget 8: 9535-9545, 2017.
16. Sun LL, Song Z, Li WZ and Tang SY: Hypoxia facilitates epithelial-mesenchymal transition-mediated rectal cancer progress. Genet Mol Res 15: gmr15048936, 2016. doi: 10.4238/gmr15048936.
17. Lehmann S, TeBoekhorst V, Odenthal J, Bianchi R, van Helvert S, Ikenberg K, Ilina O, Stoma S, Xandry J, Jiang L, *et al*: Hypoxia induces a HIF-1-dependent transition from collective-to-amoeboid dissemination in epithelial cancer cells. Curr Biol 27: 392-400, 2017.
18. Li D, Qu C, Ning Z, Wang H, Zang K, Zhuang L, Chen L, Wang P and Meng Z: Radiation promotes epithelial-to-mesenchymal transition and invasion of pancreatic cancer cell by activating carcinoma-associated fibroblasts. Am J Cancer Res 6: 2192-2206, 2016.
19. Huang W, Zhang C, Cui M, Niu J and Ding W: Inhibition of bevacizumab-induced epithelial-mesenchymal transition by BATF2 overexpression involves the suppression of Wnt/β-catenin signaling in glioblastoma cells. Anticancer Res 37: 4285-4294, 2017.
20. Bryukhovetskiy I and Shevchenko V: Molecular mechanisms of the effect of TGF-β1 on U87 human glioblastoma cells. Oncol Lett 12: 1581-1590, 2016.
21. Bryukhovetskiy A, Shevchenko V, Kovalev S *et al*: To the novel paradigm of proteome-based cell therapy of tumors: Through comparative proteome mapping of tumor stem cells and tissue-specific stem cells of humans. Cell Transplant 1 (Suppl 23): S151-S170, 2014.
22. Massagué J: TGFbeta in cancer. Cell 134: 215-230, 2008.
23. Santos JC, Ribeiro ML, Sarian LO, Ortega MM and Derchain SF: Exosomes-mediate microRNAs transfer in breast cancer chemoresistance regulation. Am J Cancer Res 6: 2129-2139, 2016.
24. Osswald M, Jung E, Sahm F, Solecki G, Venkataramani V, Blaes J, Weil S, Horstmann H, Wiestler B, Syed M, *et al*: Brain tumour cells interconnect to a functional and resistant network. Nature 528: 93-98, 2015.
25. Weil S, Osswald M, Solecki G, Grosch J, Jung E, Lemke D, Ratliff M, Hänggi D, Wick W and Winkler F: Tumor microtubes convey resistance to surgical lesions and chemotherapy in gliomas. Neuro Oncol 19: 1316-1326, 2017.
26. Sontheimer H: Brain cancer: Tumour cells on neighbourhood watch. Nature 528: 49-50, 2015.
27. Murphy SF, Varghese RT, Lamouille S, Guo S, Pridham KJ, Kanabur P, Osimani AM, Sharma S, Jourdan J, Rodgers CM, *et al*: Connexin 43 inhibition sensitizes chemoresistant glioblastoma cells to temozolomide. Cancer Res 76: 139-149, 2016.
28. Reza AM, Choi YJ, Yasuda H and Kim JH: Human adipose mesenchymal stem cell-derived exosomal-miRNAs are critical factors for inducing anti-proliferation signaling to A2780 and SKOV-3 ovarian cancer cells. Sci Rep 6: 38498, 2016.
29. Katakowski M, Buller B, Zheng X, Lu Y, Rogers T, Osobamiro O, Shu W, Jiang F and Chopp M: Exosomes from marrow stromal cells expressing miR-146b inhibit glioma growth. Cancer Lett 335: 201-204, 2013.
30. Gopal SK, Greening DW, Rai A, Chen M, Xu R, Shafiq A, Mathias RA, Zhu HJ and Simpson RJ: Extracellular vesicles: Their role in cancer biology and epithelial-mesenchymal transition. Biochem J 474: 21-45, 2017.
31. Richter N, Wendt S, Georgieva PB, Hambardzumyan D, Nolte C and Kettenmann H: Glioma-associated microglia and macrophages/monocytes display distinct electrophysiological properties and do not communicate via gap junctions. Neurosci Lett 583: 130-135, 2014.
32. Bryukhovetskiy IS, Dyuizen IV, Shevchenko VE, Bryukhovetskiy AS, Mischenko PV, Milkina EV and Khotimchenko YS: Hematopoietic stem cells as a tool for the treatment of glioblastoma multiforme. Mol Med Rep 14: 4511-4520, 2016.
33. Rappa G, Mercapide J, Anzanello F, Pope RM and Lorico A: Biochemical and biological characterization of exosomes containing prominin-1/CD133. Mol Cancer 12: 62, 2013.
34. Baumann P, Cremers N, Kroese F, Orend G, Chiquet-Ehrismann R, Uede T, Yagita H and Sleeman JP: CD24 expression causes the acquisition of multiple cellular properties associated with tumor growth and metastasis. Cancer Res 65: 10783-10793, 2005.
35. Katakowski M and Chopp M: Exosomes as tools to suppress primary brain tumor. Cell Mol Neurobiol 36: 343-352, 2016.
36. Zhou RJ, Xu XY, Liu BX, Dai WZ, Cai MQ, Bai CF, Zhang XF, Wang LM, Lin L, Jia SZ, *et al*: Growth-inhibitory and chemosensitizing effects of microRNA-31 in human glioblastoma multiforme cells. Int J Mol Med 36: 1159-1164, 2015.
37. Yarygin VN, Zaitsev AYu, Bryukhovetskiy AS, Mentkevich GL and Mheidze DM: Autologic hemopoietic stem cells preparation and method for producing, cryogenic preserving and applying it in treating traumatic nervous system disease cases. Patent RU 2283119. Filed March 29, 2005; issued September 10, 2006..